JOURNAL OF MATERIALS SCIENCE 29 (1994) 5023–5040

On the chemical vapour deposition of Ti_3SiC_2 from $TiCl_4$–$SiCl_4$–CH_4–H_2 gas mixtures

Part I *A thermodynamic approach*

C. RACAULT, F. LANGLAIS
Laboratoire des Composites Thermostructuraux (UMR-47 CNRS-SEP-UB1), Domaine Universitaire, 3 allée de La Boëtie, 33600 Pessac, France

C. BERNARD
Laboratoire de Thermodynamique et Physico-chimie Métallurgiques (URA-39), ENSEEG, Domaine Universitaire, BP 75, 38402 Saint Martin d'Hères, France

In the ternary system Ti–Si–C, the ternary compound Ti_3SiC_2 seems to exhibit promising thermal and mechanical properties. Its synthesis as a thin film from the vapour phase is very difficult owing to the complexity of the system. A contribution to the knowledge of the CVD of Ti_3SiC_2 from a $TiCl_4$–$SiCl_4$–CH_4–H_2 gas mixture is proposed on the basis of a thermodynamic approach. This approach is based on a reliable estimation of Ti_3SiC_2 thermodynamic data in good accordance with recent experimental results on its thermal stability. A first equilibrium calculation for the deposition on an inert substrate shows the influence of the experimental parameters on the composition of both the deposit and the gas phase. As a result, the deposition of Ti_3SiC_2 can be favoured by an excess of $TiCl_4$ ($\geqslant 45\%$), a rather low pressure (10–20 kPa), high temperature ($\geqslant 1273$ K) and low H_2 dilution ratio. On the basis of equilibrium calculations for various reactive substrates, complex mechanisms of Ti_3SiC_2 deposition are pointed out, with intermediate steps of substrate consumption, e.g. the formation of TiC from a carbon substrate or $TiSi_2$ from a silicon substrate.

1. Introduction

Owing to its layered crystal structure, Ti_3SiC_2 exhibits promising anisotropic properties, particularly from a thermal and mechanical point of view, with potential applications in the field of metallic and ceramic materials [1]. This ternary compound is very difficult to synthesize from the solid state as well as from the vapour phase. Only a few attempts resulted in pure Ti_3SiC_2 [1–4]. Some mechanical properties seem to depend on the synthesis method: a plastic behaviour was reported for the phase prepared by chemical vapour deposition (CVD), but was not found when Ti_3SiC_2 is obtained from solid-state diffusion. A very recent paper [4] reported that Ti_3SiC_2 exhibits a good thermal stability up to about 1300° C and an oxidation resistance better than those of titanium carbide. In order to take advantage of such properties, it was thought interesting to investigate the possibility of preparing pure and homogeneous Ti_3SiC_2 thin films from the gas phase.

The only precursor used in the previous CVD studies was a $TiCl_4$–$SiCl_4$–CCl_4–H_2 gas mixture and the conditions investigated were rather high temperatures ($T \geqslant 1473$ K) and highly diluted initial mixtures. For such a complex system, thermodynamics is a very useful tool. The only theoretical studies carried out previously in this field were based on rough estimates of thermodynamic data such as the free energy of formation of Ti_3SiC_2 which was not yet available [5, 6]. Very recently a more reliable determination of Ti_3SiC_2 data was proposed on the basis of (i) mole fraction measurements and (ii) thermodynamic models used for titanium carbide [7].

The first aim of the present paper is to propose a new estimation of the thermodynamic data of the ternary phase Ti_3SiC_2, based on the most recent experiments and models. The second purpose is to calculate the equilibrium composition of the deposited solid and the gaseous phase in the CVD system $TiCl_4$–$SiCl_4$–CH_4–H_2. The choice of CH_4 instead of CCl_4 can be justified by its lower thermal stability, which should favour Ti_3SiC_2 deposition at temperatures lower than 1473 K. The influence of the main CVD parameters (initial gaseous composition, temperature, pressure) was investigated for two cases: (i) deposition on a chemically inert substrate and (ii) deposition on silicon, carbon or silicon carbide reactive substrates. An experimental approach using CVD of Ti_3SiC_2 on the same substrates from the same precursor will be reported in a following paper [8].

0022–2461

2. Calculation procedure and thermodynamic data

The thermodynamic computations were performed by minimizing the overall Gibbs free energy of the system, both gaseous species and condensed phases being considered (Table I). The enthalpies and entropies of formation of each species were taken from the Scientific Group Thermodata Europe data bank, except for titanium silicides [9], for TiC_x [10] and for the ternary compounds of the Ti–Si–C system, i.e. $Ti_5Si_3C_x$ (T2) and Ti_3SiC_2 (T1).

2.1. Thermodynamic data of Ti_3SiC_2

Very recently Sambasivan [7] determined the free energy of formation of Ti_3SiC_2. His method is based on equilibrating Ti_3SiC_2 simultaneously with TiC_x and SiC. This equilibrium was performed by hot-pressing $TiSi_2$ and TiC_x in graphite and annealing at 1200–1500° C for several tens of hours. They determined the titanium and carbon activities by (i) measuring by electron probe microanalysis (EPMA) the stoichiometry of TiC_x near three grain junctions of SiC, TiC_x and Ti_3SiC_2 and (ii) using the thermodynamic models of Teyssandier *et al.* [11] and Urhenius [12] for the data of non-stoichiometric titanium carbide. The silicon activity was derived from the Gibbs energy of formation of silicon carbide and the carbon activity. The resulting Gibbs energy of formation ΔG_f° of Ti_3SiC_2 is given versus temperature in Fig. 1 for both models considered in the calculations. The decrease of ΔG_f° (Ti_3SiC_2) reported as the temperature increases from 1400 to 1800 K is not consistent with the decomposition experimentally found within the same temperature range [4].

TABLE I Phases considered in calculations

Solid species	Gaseous species
SiC, C, Si, $TiCl_2$, Ti $TiCl_3$, TiSi, Ti_3Si, $TiSi_2$, Ti_5Si_3, Ti_5Si_4, Ti_3SiC_2, $Ti_{0.6}Si_{0.34}C_{0.06}$	Cl_2, Ar, CHCl, H_2 CH_3Cl, CH_2Cl_2, CCl_3, $CHCl_3$, SiH_3CCl_3, CC_4, CH_4, Si_2C, C_2Cl_4, C_2H_2, C_2H_4, C_3Cl HCl, SiH_3Cl, SiCl, TiCl, SiH_2Cl_2, $SiCl_2$, $TiCl_2$, $SiHCl_3$, $SiCl_3$, $TiCl_3$, $SiCl_4$, $TiCl_4$, Si_2Cl_6, Ti_2Cl_6, H, SiH_4, Si, Ti

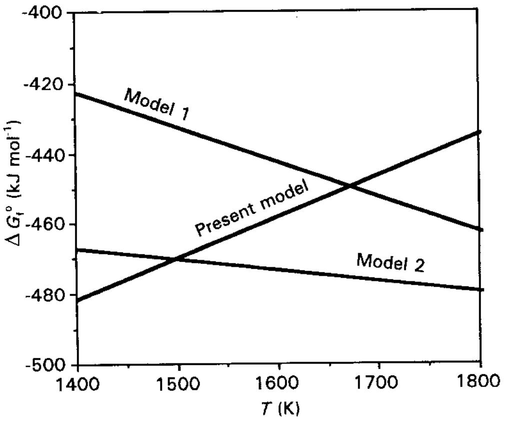

Figure 1 Variation of Ti_3SiC_2 free energy of formation with temperature according to thermodynamic models of TiC_x solid solutions from Teyssandier *et al.* [11] (model 1), Urhenius [12] (model 2) and Vincent *et al.* [10] (present model).

In the present contribution, a new calculation of ΔG_f° (Ti_3SiC_2) is proposed, based on the experimental results of Sambasivan [7] on the one hand and a more recent model for the determination of ΔG_f° (TiC_x) on the other hand. This model, from Vincent *et al.* [10], has been built up by means of the sublattice method [13]. The activities of titanium and carbon are determined by taking into account (i) the fraction Y_C of sites occupied by C atoms in the sublattice carbon/vacancies of TiC_x, expressed as

$$Y_C = \frac{X_C}{1 - X_C} \tag{1}$$

where X_C is the molar fraction of carbon in TiC_x and (ii) the interaction between a C atom and its vacancy is represented by the coefficient L_{CV}. As shown by Vincent *et al.* [10], the activity of Ti is given by

$$\begin{aligned} RT\ln a_{Ti} &= ({}^{\circ}G_{Ti}^{\mathrm{f.c.c.}} - {}^{\circ}G_{Ti}^{\beta}) \\ &\quad + RT\ln(1 - Y_C) + Y_C^2 L_{CV}^{Ti} \end{aligned} \tag{2}$$

R being the ideal gas constant and T the temperature, with

$$\begin{aligned} L_{CV}^{Ti} &= L_0 + L_1(4Y_C - 3) + L_2(2Y_C - 1)(6Y_C - 5) \\ &\quad + L_3(2Y_C - 1)^2(8Y_C - 7) \end{aligned} \tag{3}$$

$$L_0 = -89\,932.66 + 5.943\,T \tag{4}$$

$$L_1 = -28\,501 - 45.35\,T \tag{5}$$

$$L_2 = -755\,375 + 479.33\,T \tag{6}$$

$$L_3 = 699\,898 - 413.26\,T \tag{7}$$

and from Kanfman and Bernstein [14]

$${}^{\circ}G_{Ti}^{fcc} - {}^{\circ}G_{Ti}^{\beta} = -1004 + 3.766\,T \quad \mathrm{J\,mol^{-1}} \tag{8}$$

which corresponds to the Gibbs energy of formation of titanium with a hypothetical f.c.c. structure from β-titanium with b.c.c. structure. The activity of carbon is given by

$$\begin{aligned} RT\ln a_C &= \Delta G_{TiC}^{\circ} - ({}^{\circ}G_{Ti}^{\mathrm{f.c.c.}} - {}^{\circ}G_{Ti}^{\beta}) \\ &\quad + RT[\ln Y_C - \ln(1 - Y_C)] + L_{CV}^{C} \end{aligned} \tag{9}$$

with

$$\begin{aligned} L_{CV}^{C} &= L_0(1 - 2Y_C) + L_1(-1 + 6Y_C - 6Y_C^2) \\ &\quad + L_2(2Y_C - 1)(-1 + 8Y_C - 8Y_C^2) \\ &\quad + L_3(2Y_C - 1)^2(-1 + 10Y_C - 10Y_C^2) \end{aligned} \tag{10}$$

and ΔG_{TiC}° the Gibbs energy of formation of stoichiometric titanium carbide, i.e. $-160\,209\ \mathrm{J\,mol^{-1}}$ for $T > 1155$ K referred to β-Ti and C(gr) [10].

As a first approximation, the average of the carbon molar fraction measured by Sambasivan in TiC_x [7] is taken for the present determination for the temperature range investigated:

$$X_C = 0.465 \qquad (11)$$

and consequently

$$Y_C = 0.869 \qquad (12)$$

The titanium activity is then derived from Equation 2:

$$RT\ln a_{Ti} = -182\,994 + 40.347\,T \quad \mathrm{J\,mol^{-1}} \qquad (13)$$

The carbon activity is calculated according to Equation 9:

$$RT\ln a_C = 18\,547 - 40.67\,T \quad \mathrm{J\,mol^{-1}} \qquad (14)$$

The silicon activity can subsequently be derived from the free energy of formation of silicon carbide and the carbon activity, as follows:

$$RT\ln a_{Si} = \Delta G_f^\circ(\mathrm{SiC}) - RT\ln a_C \qquad (15)$$

As SiC was formed as hexagonal polytypes in the experiments of Sambasivan [7], the Gibbs energy of formation of 6H–SiC is adopted for these calculations, which results in

$$RT\ln a_{Si} = -135\,447 + 78.87\,T \quad \mathrm{J\,mol^{-1}} \qquad (16)$$

Finally, the free energy of formation of Ti_3SiC_2 can be calculated using the relation

$$\Delta G_f^\circ(\mathrm{Ti_3SiC_2}) = RT(3\ln a_{Ti} + \ln a_{Si} + 2\ln a_C) \qquad (17)$$

i.e.

$$\Delta G_f^\circ(\mathrm{Ti_3SiC_2}) = -647\,333 + 118.57\,T \quad \mathrm{J\,mol^{-1}} \qquad (18)$$

According to the present determination, Ti_3SiC_2 exhibits, in the temperature range 1400–1800 K, values of the Gibbs energy of formation which differ from those obtained previously [7] (Fig. 1). In this model, the negative entropic term results in an increase of ΔG_f° with temperature, which is in good agreement with the limited thermal stability of Ti_3SiC_2 in this temperature range.

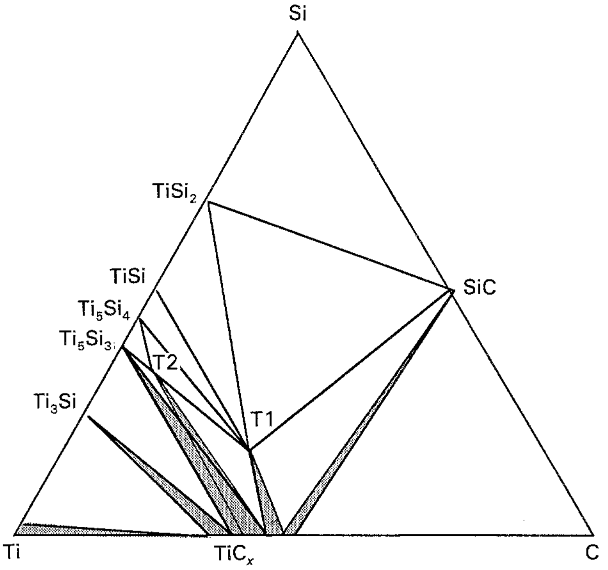

Figure 2 The phase diagram of Ti–Si–C at 1273 K calculated according to the present thermodynamic data for T1 (Ti_3SiC_2) and T2 considered as a line compound $Ti_{0.6}Si_{0.34}C_{0.05}$.

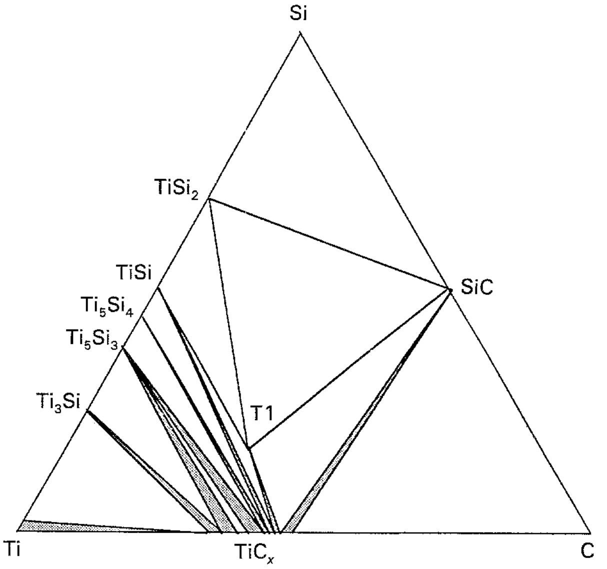

Figure 3 The phase diagram of Ti–Si–C at 1473 K calculated according to the present thermodynamic data for T1 (Ti_3SiC_2) and T2 considered as a line compound $Ti_{0.6}Si_{0.34}C_{0.05}$.

2.2. Thermodynamic data of $Ti_5Si_3C_x$

The solid solution $Ti_5Si_3C_x$, detected by Nickl *et al.* [2] from the vapour phase at 1200° C and Wakelkamp *et al.* [15] from solid-state reaction at 1250° C, has not yet been characterized, e.g. in terms of thermal stability, and no thermodynamic data are available. Above these temperatures, neither Ti_5Si_3 nor $Ti_5Si_3C_x$ was identified by Goto and Hirai [3] in their synthesis from the gas mixture $TiCl_4$–$SiCl_4$–CCl_4–H_2.

Consequently, a simplified determination of the thermodynamic data of $Ti_5Si_3C_x$ is presently proposed. The solid solution is replaced by a line compound $Ti_{0.6}Si_{0.34}C_{0.05}$ whose thermodynamic data are estimated as for a mixture of 1 mol of Ti_3SiC_2 and 4 mol of Ti_5Si_3, i.e. for $T > 1155$ K

$$\Delta G_f^\circ(\mathrm{Ti_{0.6}Si_{0.34}C_{0.05}}) = -81\,681 + 5.579\,T \quad \mathrm{J\,mol^{-1}} \qquad (19)$$

From this value and the data of Ti_3SiC_2 previously assessed, the ternary phase diagram of Ti–Si–C at 1273 K can be calculated and is shown in Fig. 2. If these calculations are carried out at 1473 K, the phase T2 derived from Ti_5Si_3 is no longer present (Fig. 3).

In order to test the sensitivity of this phase to the corresponding data, the phase diagram has been calculated on the basis of a compound $Ti_{0.6}Si_{0.34}C_{0.05}$ stabilized by 10 kJ mol^{-1}, i.e.

$$\Delta G_f^\circ(\mathrm{Ti_{0.6}Si_{0.34}C_{0.05}}) = -91\,681 + 5579\,T \quad \mathrm{J\,mol^{-1}} \qquad (20)$$

In this case, at 1273 K the ternary diagram (Fig. 4) is very similar to those experimentally derived by Wakelkamp *et al.* [15] but $Ti_{0.6}Si_{0.34}C_{0.05}$ is stable up to 1573 K while Ti_3SiC_2 is already decomposed. This result shows that the stability of the solid solution and consequently the phase diagram in the Ti-rich region are highly sensitive to the thermodynamic

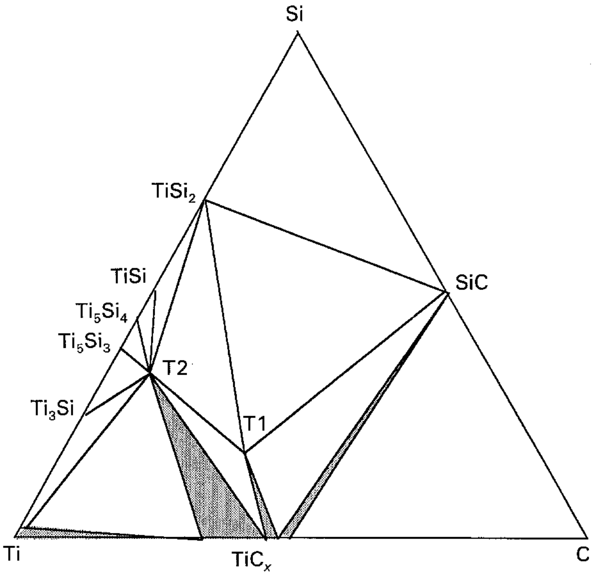

Figure 4 The phase diagram of Ti–Si–C at 1273 K calculated according to the present thermodynamic data for T1 (Ti_3SiC_2) and T2 considered as a line compound $Ti_{0.6}Si_{0.34}C_{0.05}$ stabilized by $10\ kJ\ mol^{-1}$.

data chosen for $Ti_5Si_3C_x$, which have to be accurately determined on the basis of experimental investigations.

In the following, the Gibbs energy of formation according to Equation 19 is taken for the solid solution $Ti_5Si_3C_x$.

3. CVD of Ti_3SiC_2 from the $TiCl_4$–$SiCl_4$–CH_4–H_2 system on a chemically inert substrate

The experimental parameters introduced in the present equilibrium calculations are, on the one hand, composition parameters, i.e. the ternary composition given by the initial molar fractions x_{TiCl_4}, x_{SiCl_4} and x_{CH_4} and the dilution ratio defined by $\alpha = x_{H_2}/(x_{TiCl_4} + x_{SiCl_4} + x_{CH_4})$ (with $5 \leqslant \alpha \leqslant 100$); on the other hand, total pressure ($2 \leqslant P \leqslant 50$ kPa) and temperature ($1073 \leqslant T \leqslant 1473$ K) are considered. The computation results performed according to MELANGE software [16] show that the following solid phases can be present in significant amounts at equilibrium: the ternary compound Ti_3SiC_2, TiC, SiC, three titanium silicides $TiSi_2$, Ti_5Si_4 and TiSi, and to a lesser extent free carbon and free silicon. In order to show the influence of the initial ternary composition on the equilibrium composition of the solid, various circles are located at different positions in the ternary diagram (x_{TiCl_4}–x_{SiCl_4}–x_{CH_4}) and these circles are filled by sectors corresponding to the relative amounts of the various present phases (Fig. 5). The grey levels associated to the solid species are listed in Table 2. The thermodynamic yields for these various phases are calculated according to the following equations:

$$\eta_{Ti}(Ti_xSi_yC_z) = 100\,\frac{x n^{eq}_{Ti_xSi_yC_z}}{n^{in}_{TiCl_4}}. \tag{21}$$

with respect to Ti and

$$\eta_{Si}(Ti_xSi_yC_z) = 100\,\frac{y n^{eq}_{Ti_xSi_yC_z}}{n^{in}_{SiCl_4}}. \tag{22}$$

with respect to Si, when n^{eq} and n^{in} mean equilibrium and initial mole numbers, respectively.

3.1. Influence of the composition of the gaseous precursor

Fig. 5 gives the equilibrium composition of the deposit for various initial gaseous mixtures, various dilution ratios, a temperature of 1273 K and a total pressure of 20 kPa. A gas phase rich in $TiCl_4$ and rather depleted in CH_4 is favourable to Ti_3SiC_2 deposition. Low values of α result in rather pure deposits, particularly of SiC, while high α values result in complex co-deposits made of three phases in most cases. In the ternary CVD diagram ($TiCl_4$–$SiCl_4$–CH_4), the domain of composition which gives rise to Ti_3SiC_2 as a pure phase or part of a co-deposit becomes larger as the dilution ratio α increases, but at the same time the purity of the ternary phase decreases. The best dilution conditions are $10 \leqslant \alpha \leqslant 20$, where a pure Ti_3SiC_2 deposition can occur in a significant range of ternary composition, around 80% $TiCl_4$, 10% $SiCl_4$, 10% CH_4.

For this specific initial ternary composition, the thermodynamic yields of solid phases are reported in Fig. 6. The yield of Ti_3SiC_2 with respect to Ti increases rapidly from about 4% to about 19% when α is raised from 5 to 10 (Fig. 6a). For $\alpha \geqslant 10$, η_{Ti} (Ti_3SiC_2) remains at the same level, but the silicide Ti_5Si_4 occur simultaneously for very high dilution ratios ($\alpha \geqslant 50$). The yield of Ti_3SiC_2 with respect to Si exhibits the same behaviour as a function of α, with a rapid increase from 10 to 50% as α increases from 5 to 10 and then a constant value of 50% (Fig. 6b). These yield calculations confirm the best α range ($10 \leqslant \alpha \leqslant 20$) where Ti_3SiC_2 can be deposited as a pure phase with the highest yield.

For the same conditions of initial ternary composition, total pressure and temperature, the equilibrium partial pressures of the gas phase are drawn as a function of the dilution ratio α in Fig. 7. An increase of α results in an increase of H_2 partial pressure and consequently a decrease of almost all the other partial pressures. Besides HCl which is a deposition reaction product, the dominant species occurring at equilibrium are the titanium chlorides $TiCl_4$ and $TiCl_3$, which is consistent with the rather low thermodynamic yields of the solid phases with respect to Ti. The chlorosilanes exhibit much lower equilibrium partial pressures, their consumption by the deposition reactions resulting in higher yields with respect to Si. Finally, the very low level of CH_4 and other hydrocarbons means the quasi-total consumption of this species and a yield of solid phases with respect to C very close to 100%.

3.2. Influence of the total pressure

In order to investigate if the deposition domain of Ti_3SiC_2 can be enlarged by varying the total pressure, two values of α ratio were chosen: the first one, $\alpha = 10$, a low dilution rather favourable to the formation of

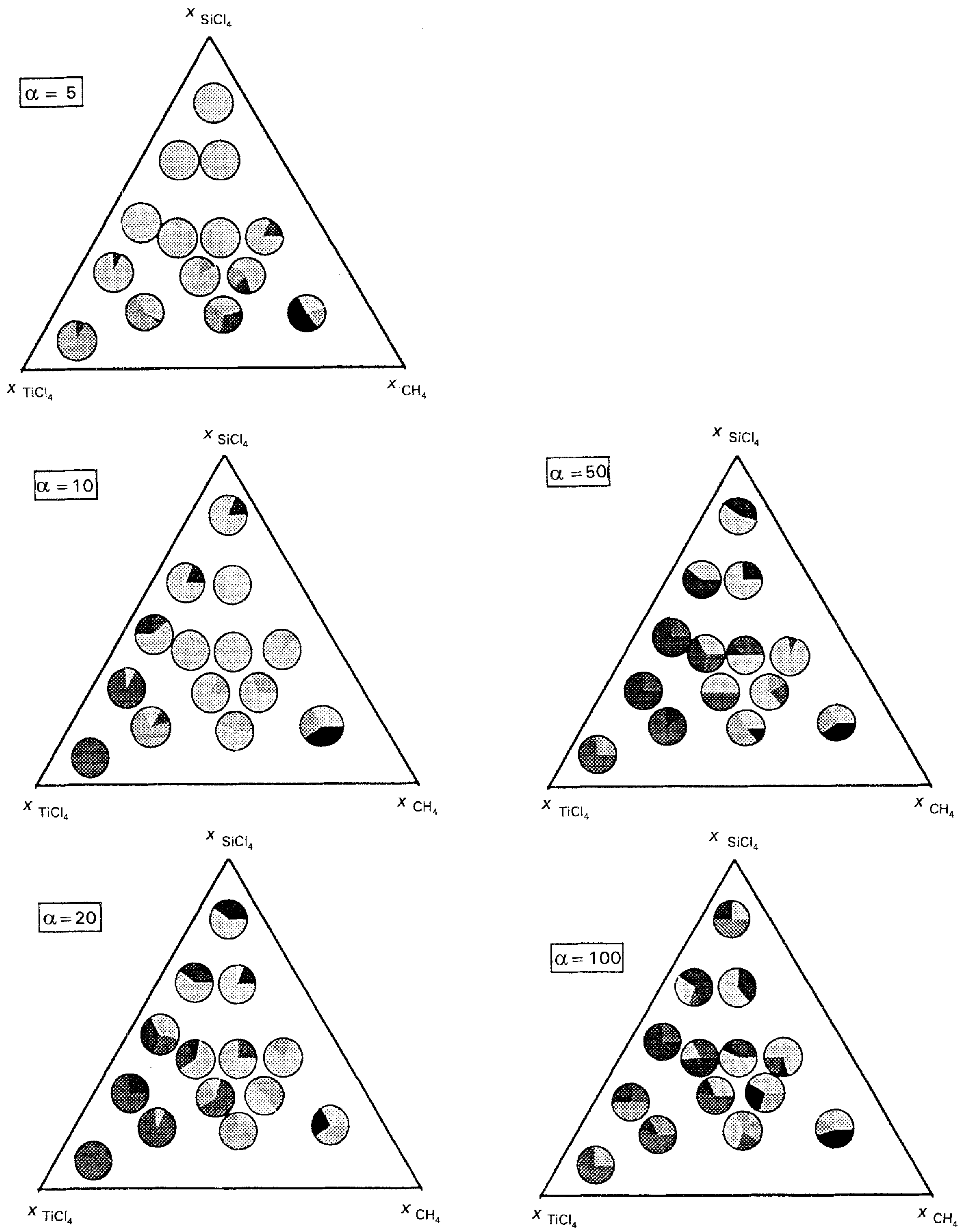

Figure 5 Influence of the initial gaseous mixture on the equilibrium composition of the solid for $P = 20$ kPa, $T = 1273$ K and various dilution ratios.

Ti_3SiC_2 and the second one, $\alpha = 50$, a high dilution that is rather unfavourable.

Fig. 8 gives the influence of the total pressure in the range 2–50 kPa on the equilibrium composition of the deposit for various initial gaseous mixtures, a temperature of 1273 K and both α values previously defined. The ternary composition domain favourable to Ti_3SiC_2 is reduced by raising the total pressure for $\alpha = 10$. No pure Ti_3SiC_2 can be obtained at $P = 50$ kPa, while for lower pressures a significant range of ternary composition gives rise to pure Ti_3SiC_2 deposition. For the high dilution ratio ($\alpha = 50$), the total pressure has no great influence on the occurrence domain of Ti_3SiC_2. Its purity is only slightly increased by increasing the deposition pressure.

For the low dilution ratio $\alpha = 10$, two initial ternary compositions which can give rise to pure Ti_3SiC_2 are interesting to be studied in more detail, i.e. in terms of thermodynamic yields. For the first one (80% $TiCl_4$, 10% $SiCl_4$, 10% CH_4), the yields of the solid phases are reported in Fig. 9 as a function of the

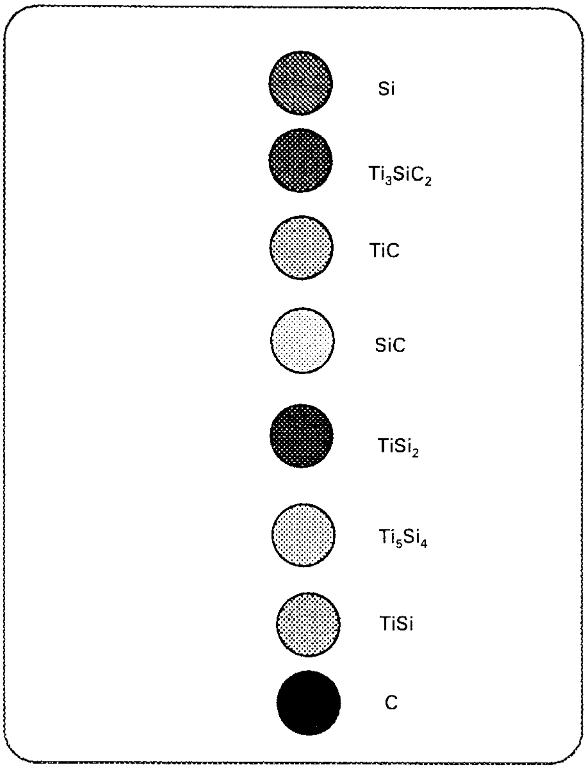

TABLE II

total pressure. The yield of Ti_3SiC_2 with respect to Ti is constant at about 19% without other solid phases for $P \leqslant 20$ kPa. Above this pressure value, a co-deposition of Ti_3SiC_2–TiC with a slight decrease of the Ti_3SiC_2 yield occurs. For the second ternary composition studied (60% $TiCl_4$, 30% $SiCl_4$, 10% CH_4), the thermodynamic yields with respect to Si are represented versus P in Fig. 10. The Ti_3SiC_2 yield decreases from 17 to 12% when the pressure increases from 10 to 50 kPa. The ternary phase is pure only in the range 10–20 kPa. Below 10 kPa a co-deposit with $TiSi_2$ occurs and above 20 kPa, SiC is co-deposited with Ti_3SiC_2.

For the high dilution ratio $\alpha = 50$, the following ternary composition which can give rise to the largest amount of Ti_3SiC_2 is chosen: 60% $TiCl_4$, 20% $SiCl_4$, 20% CH_4. Under these conditions the variations of the thermodynamic yields versus total pressure (Fig. 11) point out the relative importance of the phases co-deposited with Ti_3SiC_2, i.e. TiSi and $TiSi_2$ at low pressures ($P \leqslant 10$ kPa) and only $TiSi_2$ at higher pressures. The favourable effect of increasing pressure is also evidenced: the yield of Ti_3SiC_2 remains at a level of 50% over the whole pressure range while those of the other phases decrease continuously. For the highest investigated pressure, i.e. 50 kPa, an almost pure Ti_3SiC_2 deposit is predicted by the thermodynamic approach.

3.3. Influence of the temperature

The influence of the deposition temperature on the equilibrium composition of the solid, and thermodynamic yields and the partial pressures of the gaseous species, was investigated for a pressure of 20 kPa and a dilution ratio $\alpha = 20$.

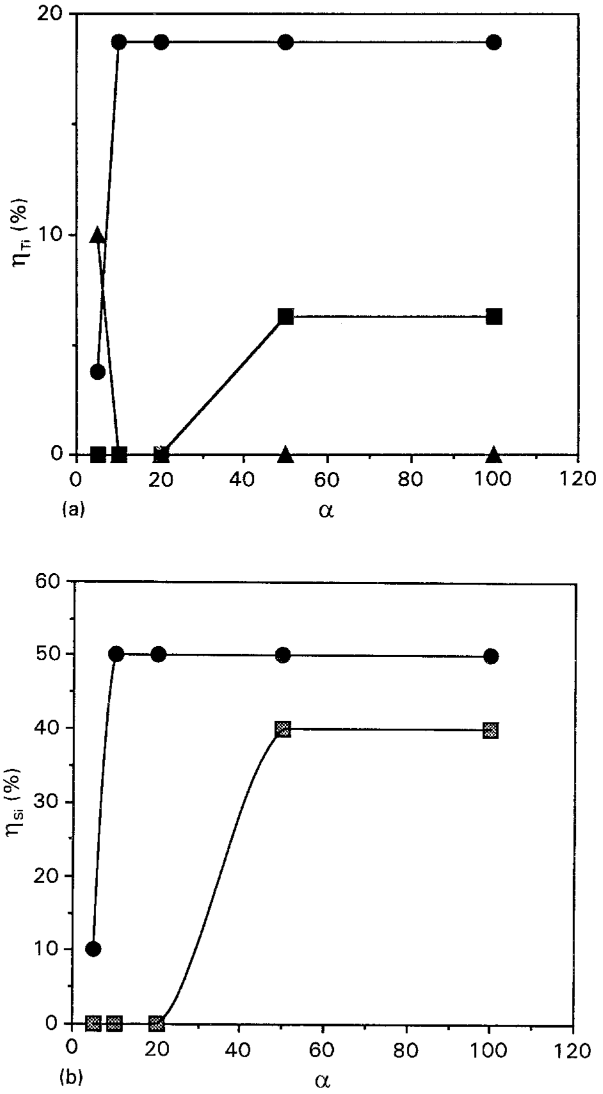

Figure 6 Influence of the dilution ratio α on the thermodynamic yields to the solid phases at equilibrium, calculated with respect to (a) titanium and (b) silicon, for $T = 1273$ K, $P = 20$ kPa and the initial composition 80% $TiCl_4$, 10% $SiCl_4$, 10% CH_4; (▲) TiC, (●) Ti_3SiC_2, (■) Ti_5Si_4.

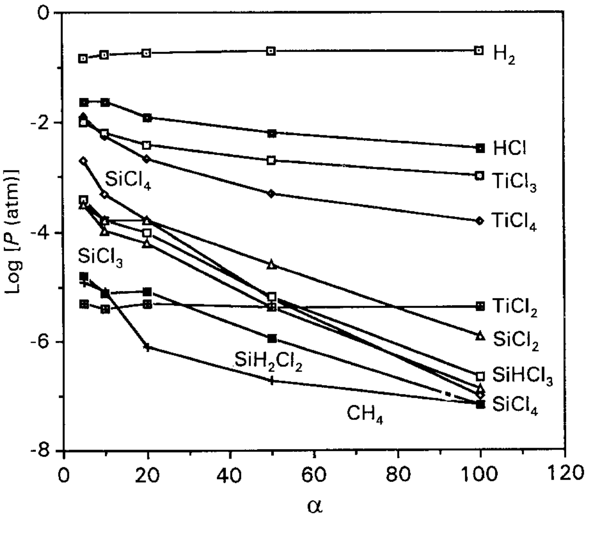

Figure 7 Influence of the dilution ratio α on the equilibrium partial pressures for $T = 1273$ K, $P = 20$ kPa and the initial composition 80% $TiCl_4$, 10% $SiCl_4$, 10% CH_4.

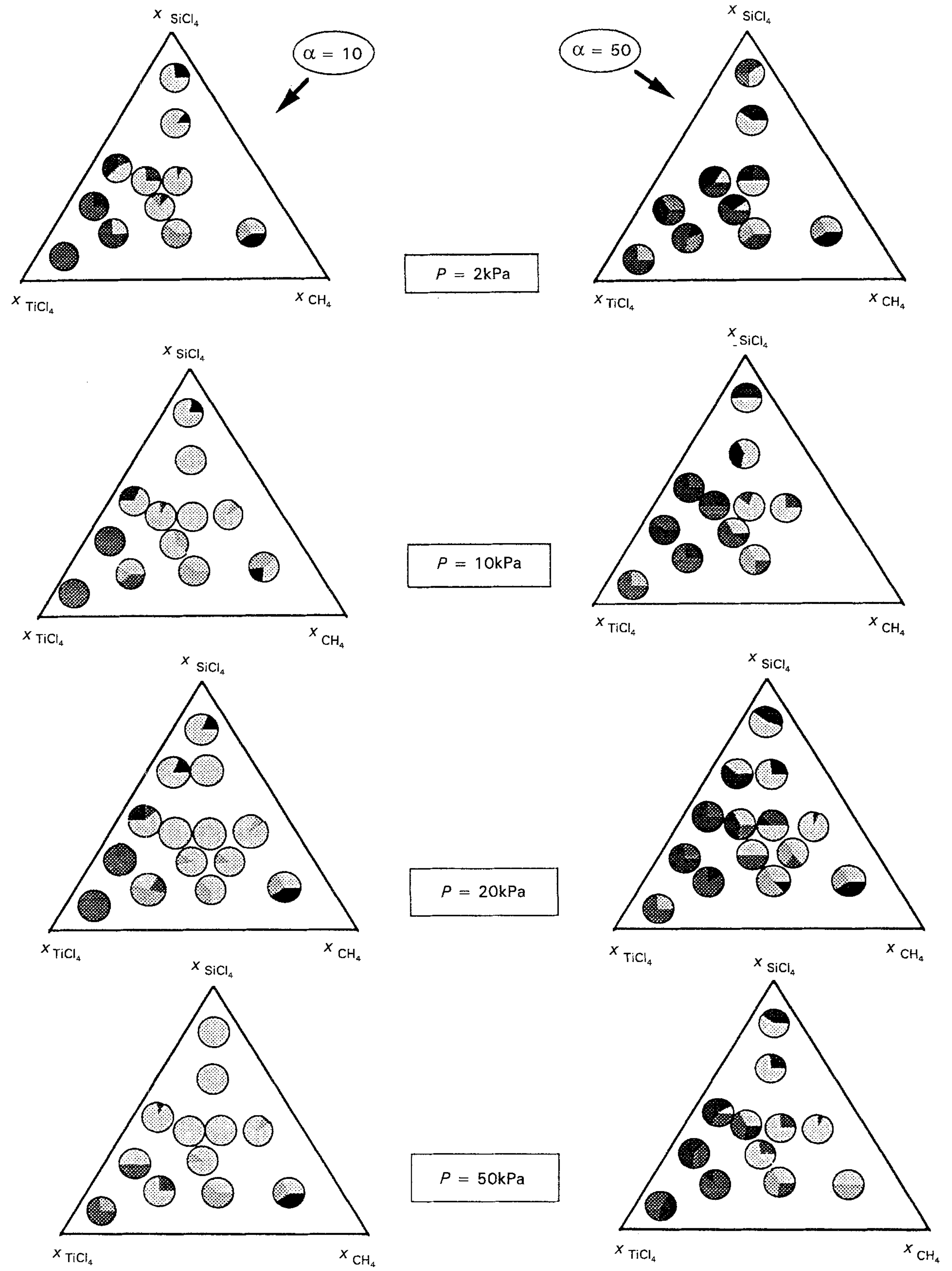

Figure 8 Influence of the initial gaseous mixture on the equilibrium composition of the solid for $T = 1273$ K, $\alpha = 10$ and 50 and various total pressures. For key to sectors see Table 2.

Fig. 12 shows that an increase of the temperature enlarges the Ti_3SiC_2 occurrence domain, particularly between 1073 and 1173 K. The ternary composition (80% $TiCl_4$, 10% $SiCl_4$, 10% CH_4) is chosen again to study the thermodynamic yields versus temperature (Fig. 13). Above 1173 K the Ti_3SiC_2 yield is constant, i.e. about 19% with respect to Ti and 50% with respect to Si. Below 1173 K, both Ti_3SiC_2 yields are lower and a co-deposition with a large amount of TiC is predicted. Between 1173 and 1473 K, Ti_3SiC_2 is

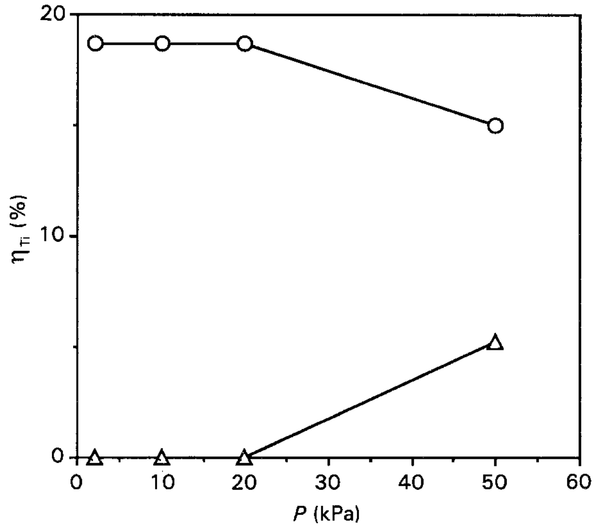

Figure 9 Influence of the total pressure on the thermodynamic yields of the solid phases at equilibrium, calculated with respect to titanium, for $T = 1273$ K, $\alpha = 10$ and the initial composition 80% $TiCl_4$, 10% $SiCl_4$, 10% CH_4: (△) TiC, (○) Ti_3SiC_2.

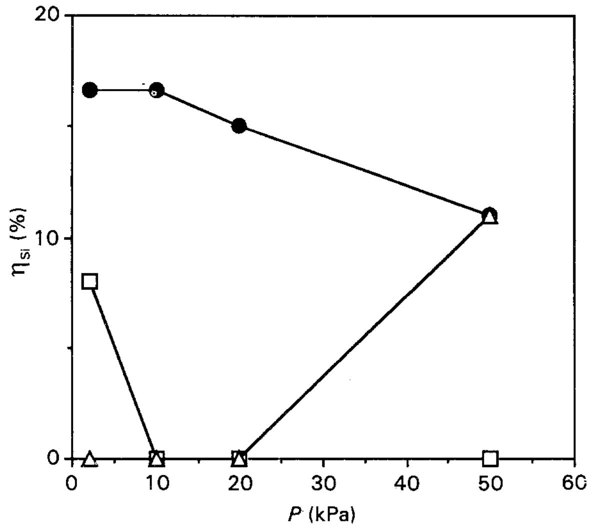

Figure 10 Influence of the total pressure on the thermodynamic yields of the solid phases at equilibrium, calculated with respect to silicon, for $T = 1273$ K, $\alpha = 10$ and the initial composition 60% $TiCl_4$, 30% $SiCl_4$, 10% CH_4; (△) SiC, (□) $TiSi_2$, (●) Ti_3SiC_2.

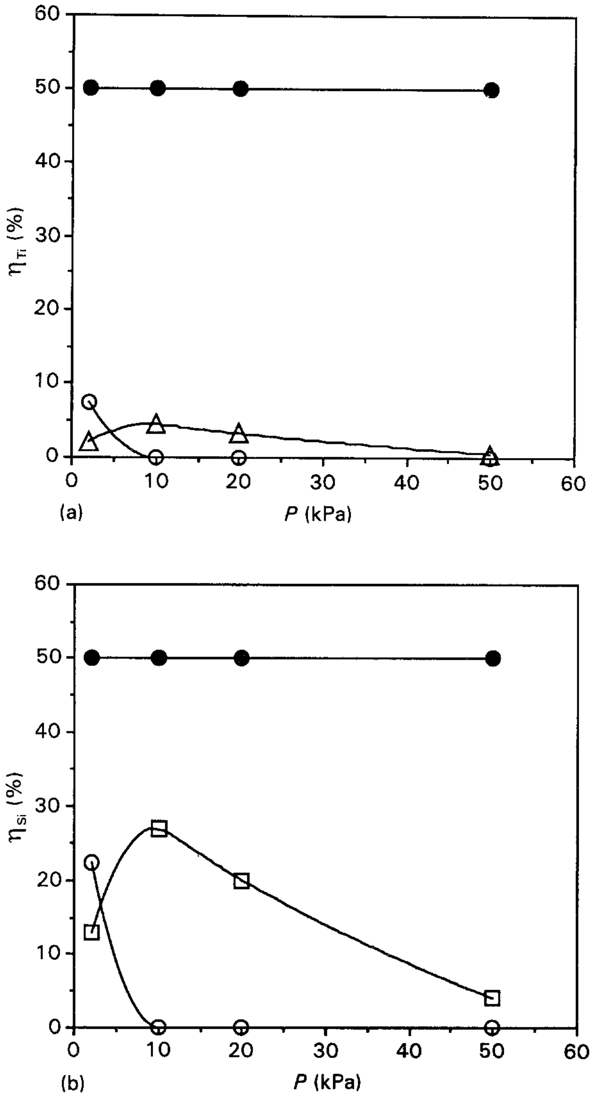

Figure 11 Influence of the total pressure on the thermodynamic yields of the solid phases at equilibrium, calculated with respect to (a) titanium and (b) silicon, for $T = 1273$ K, $\alpha = 50$ and the initial composition 60% $TiCl_4$, 20% $SiCl_4$, 20% CH_4; (○) TiSi, (□, △) $TiSi_2$, (●) Ti_3SiC_2.

found to be pure except at about 1373 K where TiSi can act as an impurity. The equilibrium partial pressures are reported as a function of temperature in Fig. 14. The respective values for HCl, titanium chlorides, chlorosilanes and CH_4 can explain the different thermodynamic yields with respect to Ti and Si. On the other hand, when the temperature increases, $TiCl_4$ and $SiCl_4$ are replaced by sub-chlorides such as $TiCl_3$, $SiCl_2$ and $SiCl_3$.

The influence of temperature was also investigated for two types of condition: the first one rather unfavourable to Ti_3SiC_2 deposition i.e. $P = 50$ kPa, $\alpha = 10$; the second one rather favourable, i.e. $P = 50$ kPa, $\alpha = 50$ (Fig. 15). In the first case an increase of temperature enhances the stability of Ti_3SiC_2, which is predicted to be deposited as a pure phase at 1473 K for the ternary composition 60% $TiCl_4$, 30% $SiCl_4$, 10% CH_4. In the second case, pure Ti_3SiC_2 is highly favoured by decreasing temperature. For $T = 1073$ K, $P = 50$ kPa and $\alpha = 50$ a relatively large domain of ternary composition is favourable to pure Ti_3SiC_2: $0.45 \leqslant x_{TiCl_4} \leqslant 0.8$; $0.1 \leqslant x_{SiCl_4} \leqslant 0.45$; $x_{CH_4} = 10$.

3.4. Discussion

These various results of thermodynamic calculations permit one to give tendencies for the influence of experimental parameters on the deposition of Ti_3SiC_2. The best conditions in terms of initial ternary composition are an excess of $TiCl_4$ (more than 45%), a limited $SiCl_4$ fraction (less than 45%) and a small CH_4 fraction (lower than 20%). In terms of dilution ratio α in H_2, an intermediate value of about 10–20 is favourable. The influence of deposition pressure and temperature depends on the values of the other parameters. A pure Ti_3SiC_2 deposition is favoured by

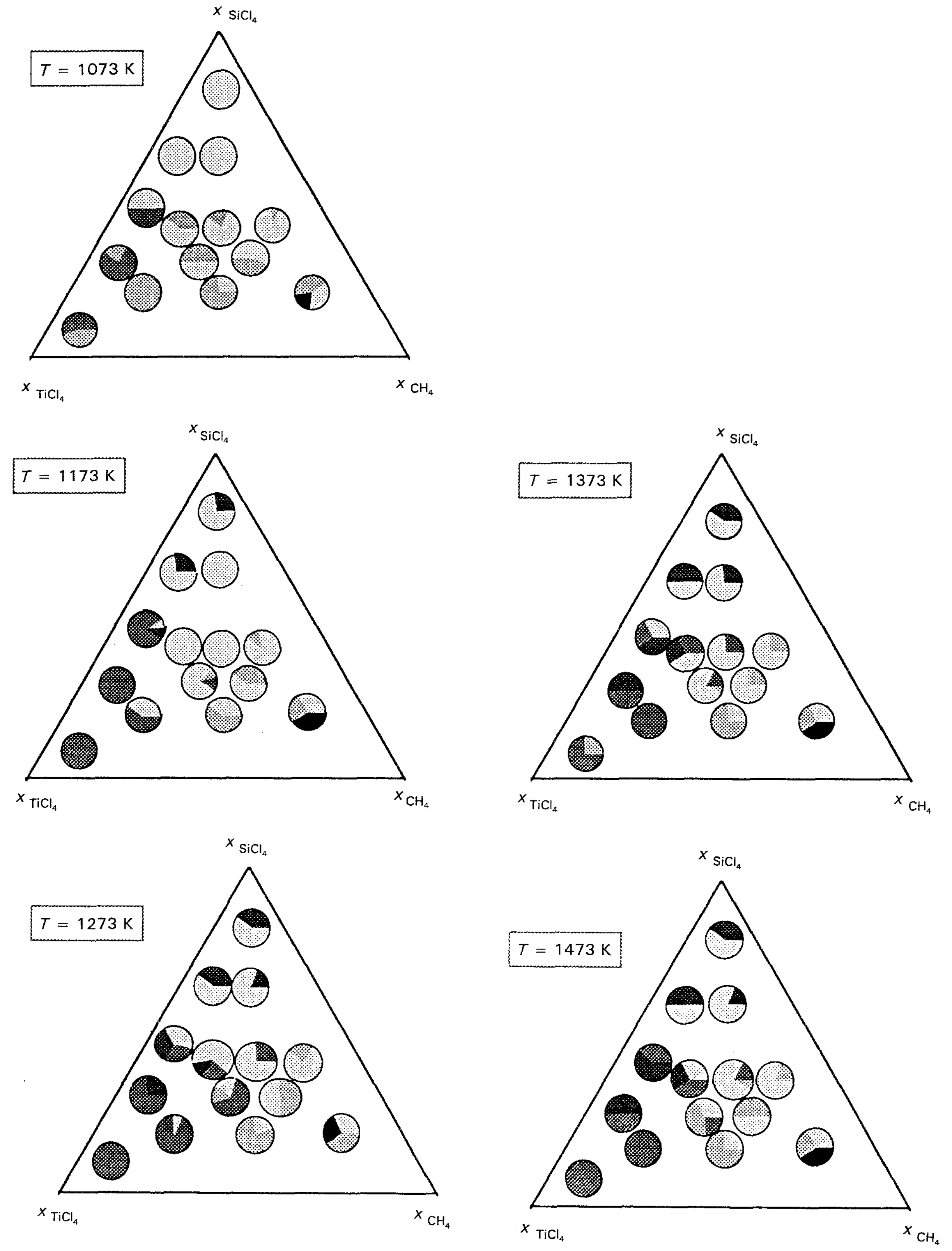

Figure 12 Influence of the initial gaseous mixture on the equilibrium composition of the solid for $P = 20$ kPa, $\alpha = 20$ and various temperatures. For key to sectors see Table 2.

a rather low pressure (10–20 kPa) for a low dilution ratio ($\alpha = 50$). Finally, the stability of Ti_3SiC_2 is enhanced by increasing the temperature for most conditions of pressure and dilution, except for high pressure ($P \geqslant 50$ kPa) and high dilution ratio ($\alpha \geqslant 50$) where Ti_3SiC_2 is favoured by decreasing the temperature down to 1073 K.

The most probable overall reaction giving rise to Ti_3SiC_2 corresponds to the equation

$$3TiCl_4 + SiCl_4 + 2CH_4 + 4H_2 \rightarrow Ti_3SiC_2 + 16HCl \quad (23)$$

With respect to the stoichiometric composition corresponding to this equation, a large excess of $TiCl_4$

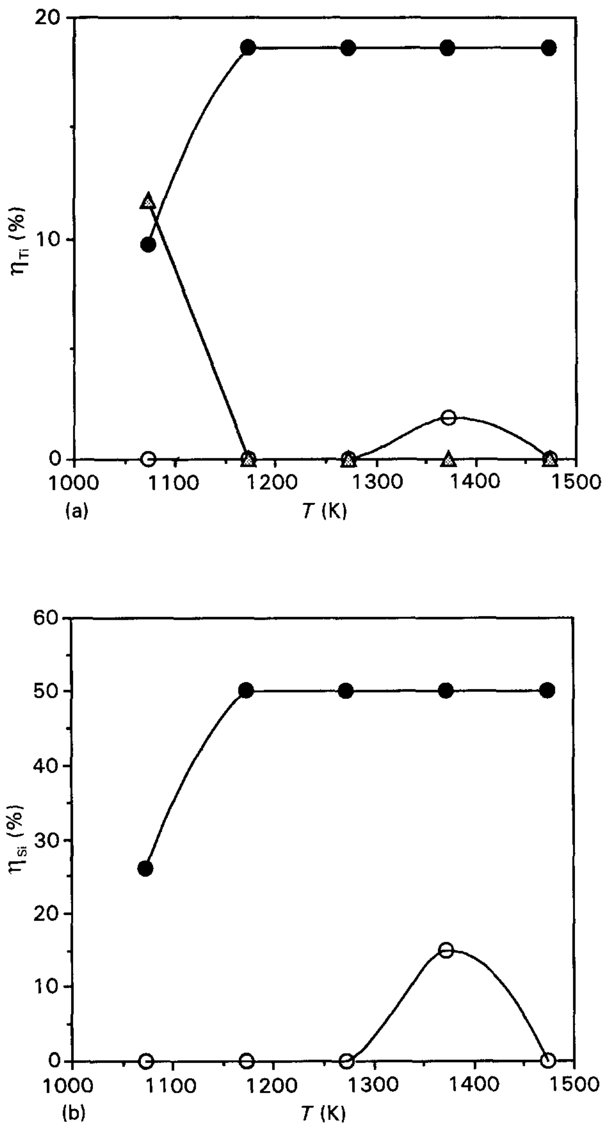

Figure 13 Influence of the temperature on the thermodynamic yields of the solid phases at equilibrium, calculated with respect to (a) titanium and (b) silicon, for $P = 20$ kPa, $\alpha = 20$ and the initial composition 80% $TiCl_4$, 10% $SiCl_4$, 10% CH_4; (△) TiC, (○) TiSi, (●) Ti_3SiC_2.

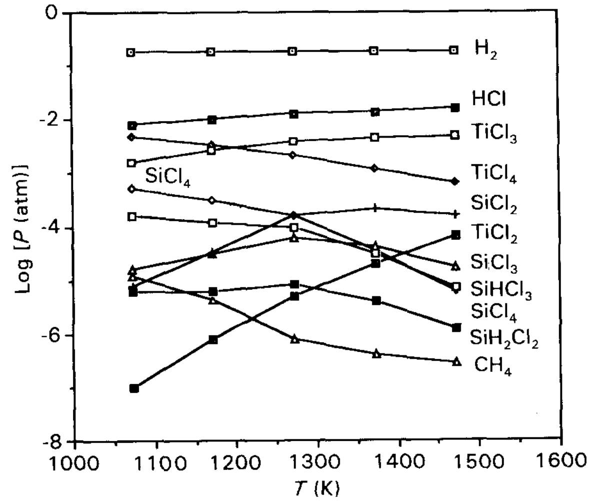

Figure 14 Influence of the temperature of the equilibrium partial pressures for $P = 20$ kPa, $\alpha = 20$ and the initial composition 80% $TiCl_4$, 10% $SiCl_4$, 10% CH_4.

and H_2 and a small excess of $SiCl_4$ are needed to deposit pure Ti_3SiC_2. In this case, the only other reactions involved in the system are homogeneous reactions, e.g. reduction of $TiCl_4$ and $SiCl_4$ by H_2, resulting in sub-chloride formation. Owing to these secondary reactions, the thermodynamic yields are lower than 20% with respect to Ti and 50% with respect to Si. A very high dilution in H_2 is not only favourable to Ti_3SiC_2 and various gaseous sub-chlorides, but also to the deposition of silicides, e.g. according to the reactions

$$TiCl_4 + SiCl_4 + 4H_2 \rightarrow TiSi + 8HCl \quad (24)$$

$$TiCl_4 + 2SiCl_4 + 6H_2 \rightarrow TiSi_2 + 12HCl \quad (25)$$

To prevent a co-deposition of Ti_3SiC_2 with silicides, the dilution must not be too high and limited to values between 10 and 20.

4. CVD of Ti_3SiC_2 from the $TiCl_4$–$SiCl_4$–CH_4–H_2 system on reactive substrates

In order to simulate the role played by the usual substrates on which Ti_3SiC_2 could be deposited, the thermodynamic approach was carried out by introducing an excess of the substrate material in the initial composition, as previously reported for other CVD systems [17, 18]. Moreover, to understand the possible steps of the deposition process, successive equilibrium calculations were performed by taking as substrate at each step the complex solid formed at the previous step. The last step is reached when the nature and relative amounts of the various solid phases are not changed in the equilibrium calculations, i.e. when the solid phases introduced become inert with respect to the gas phase.

4.1. Carbon substrate

The equilibrium calculations carried out with an excess of solid carbon show that this substrate is etched except for CH_4-rich gaseous mixtures, which result in a slight carbon deposition. This consumption of carbon is detailed as a function of the initial composition for two dilution ratios ($\alpha = 20$ and 100), a temperature of 1273 K, a pressure of 20 kPa and a high enough excess of carbon (Fig. 16). The only composition parameters which influence the carbon etching are the CH_4 molar fraction and the dilution ratio α. A decrease of x_{CH_4} and an increase of α favour the consumption of carbon in accordance with the following equations:

$$C + 2H_2 \rightarrow CH_4 \quad (26)$$

$$TiCl_4 + C + 2H_2 \rightarrow TiC + 4HCl \quad (27)$$

$$SiCl_4 + C + 2H_2 \rightarrow SiC + 4HCl \quad (28)$$

Another representation of the behaviour of a reactive carbon substrate is given by Fig. 17. A carbon yield defined by

$$\eta_C = 100 \frac{n_C^{eq} - n_C^{in}}{n_C^{in} + n_{CH_4}^{in}} \quad (29)$$

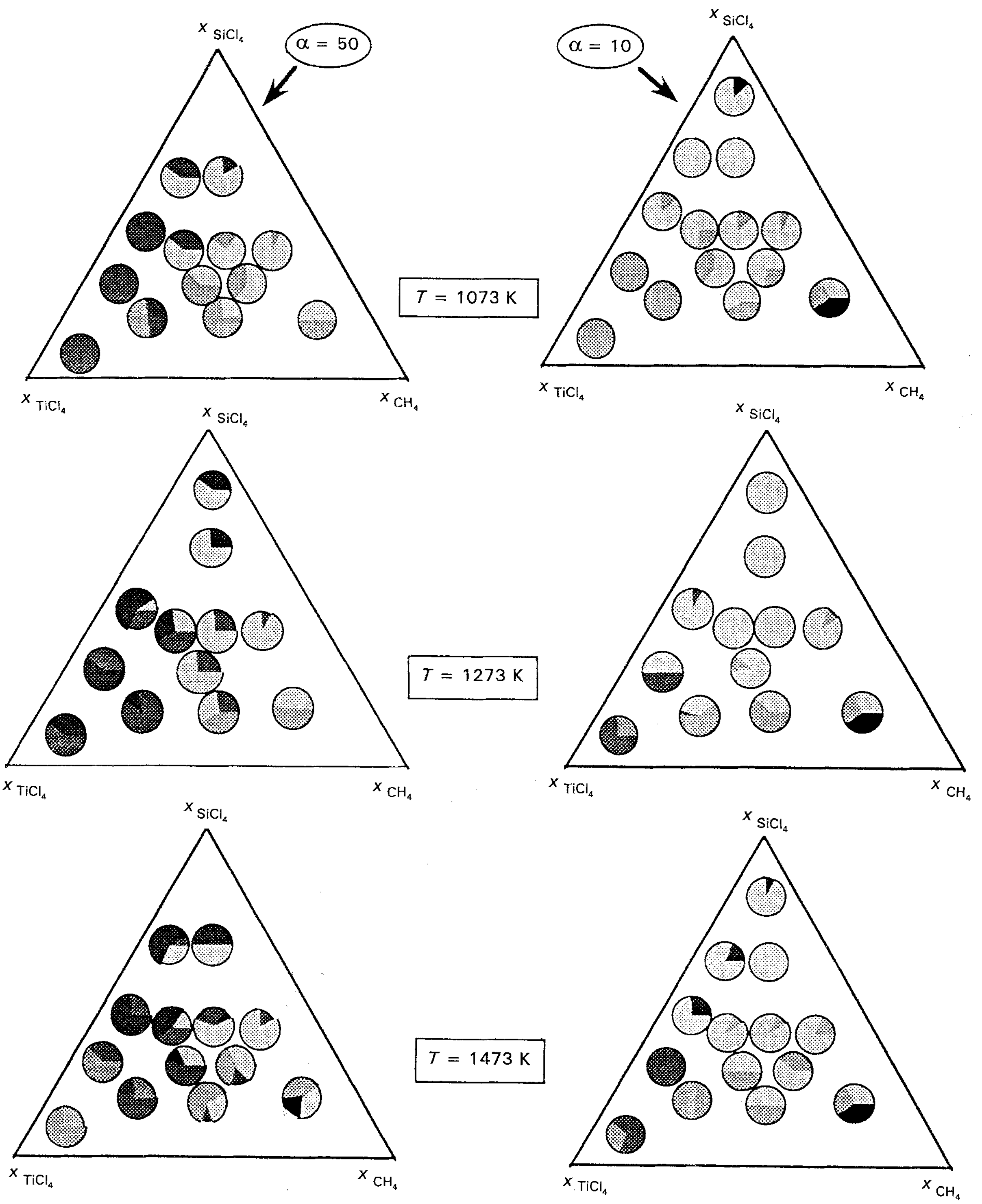

Figure 15 Influence of the initial gaseous mixture on the equilibrium composition of the solid for $P = 50$ kPa, $\alpha = 10$ and 50 and various temperatures. For key to sectors see Table 2.

is drawn versus x_{CH_4} for $\alpha = 20$ and $\alpha = 100$. A CH_4 molar fraction higher than 0.55 is needed to prevent a carbon consumption.

The influence of the gas phase composition on the nature of the solid formed at equilibrium is given in Fig. 18 for $T = 1273$ K, $P = 20$ kPa and $\alpha = 20$ and 100. The results corresponding to the first equilibrium calculation confirm that Equations 27 and 28 for TiC and SiC formation contribute highly to the carbon consumption occurring in a large range of initial compositions (Fig. 18a$_1$ and b$_1$). If the amount of TiC is obviously increased by increasing the $TiCl_4$ molar fraction, it is also slightly favoured with respect to SiC by increasing the dilution ratio α.

By taking the various two-phase solids obtained in this first step as substrate, new equilibrium calculations with the same corresponding initial gaseous mixtures show that Ti_3SiC_2 can be formed by consuming the TiC–SiC mixtures (Fig. 18a$_2$ and b$_2$). For compositions with a high $TiCl_4$ mole fraction, Ti_3SiC_2 can be formed as a pure phase, particularly for a high dilution ratio ($\alpha = 100$). If a third series of calculations

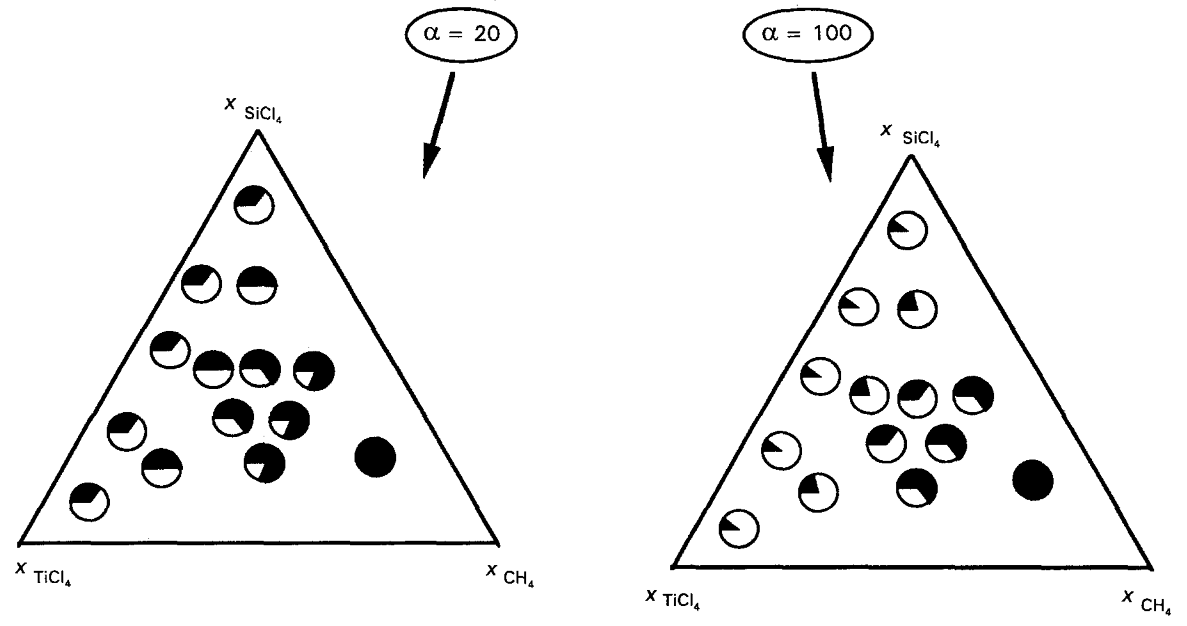

Figure 16 Influence of the initial gaseous mixture on the extent of the consumption of a carbon substrate at equilibrium for $T = 1273$ K, $P = 20$ kPa, $\alpha = 20$ and 100; $n(C) = 10$ mol, $n(SiCl_4) + n(TiCl_4) + n(CH_4) = 10$ mol. Clear sectors represent the amount of consumed substrate and dark sectors the amount of unetched substrate.

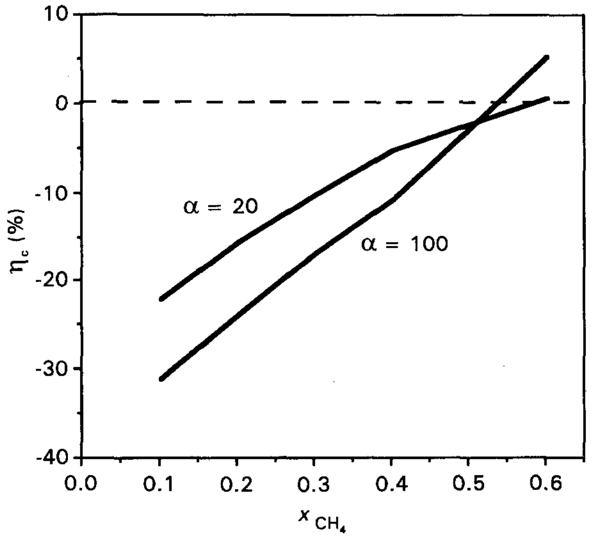

Figure 17 Influence of CH_4 initial molar fraction on the carbon thermodynamic yields for $T = 1273$ K, $P = 20$ kPa, $\alpha = 20$ and 100.

is carried out by taking as substrate the solids obtained in the second step, these solids are not affected by the chemical reactions; thus they can be considered as inert substrates and the compositions of the finally obtained deposits are identical to those previously calculated for an inert substrate (Fig. 18a$_3$ and b$_3$ and Fig. 5). On the basis of these results, Ti_3SiC_2 can be deposited on a carbon substrate only after an intermediate stage corresponding mainly to a consumption of carbon by $TiCl_4$ giving rise to TiC (Equation 27). An intermediate formation of SiC is much less favourable to Ti_3SiC_2 deposition.

For an initial composition of the gas phase favourable to Ti_3SiC_2 formation, i.e. $x_{TiCl_4} = 80\%$, $x_{SiCl_4} = 10\%$ and $x_{CH_4} = 10\%$, the equilibrium partial pressures of the gas phase are given in Fig. 19 for the first two steps previously defined and two values of the dilution ratio ($\alpha = 20$ and 100). For $\alpha = 20$, the first step of the deposition process involves a consumption of $TiCl_4$, $SiCl_4$ and CH_4, while a small amount of $TiCl_3$ is produced in addition to HCl. These results are in good agreement with Equation 27 for TiC formation. Other reactions must be considered to occur, such as

$$SiCl_4 + CH_4 \rightarrow SiC + 4HCl \qquad (30)$$

$$TiCl_4 + \tfrac{1}{2}H_2 \rightarrow TiCl_3 + HCl \qquad (31)$$

At the second step, CH_4 and $SiCl_4$ are totally consumed and $TiCl_4$ only partially, the subchloride $TiCl_3$ occurring again besides HCl. The main reaction involved is the formation of Ti_3SiC_2 from TiC and the three source species. For the high dilution ratio $\alpha = 100$, the equilibrium gas phase composition contains only HCl and a small amount of CH_4 at the first step. It means that all the reactions 26 to 28 occur with consumption of carbon and production of TiC and SiC. At the second step, the subchloride $TiCl_3$ and to a lesser extent $TiCl_4$ are present with HCl, which corresponds to reactions giving rise to Ti_3SiC_2 from TiC or SiC.

4.2. Silicon substrate

As shown by the results of the equilibrium calculations carried out with an excess of solid silicon, this substrate can be highly consumed, except for $SiCl_4$-rich gaseous mixtures. Fig. 20 shows the influence of the initial composition on this consumption for $T = 1273$ K, $P = 20$ kPa and $\alpha = 20$ and 100 and a high enough excess of silicon. The extent of the

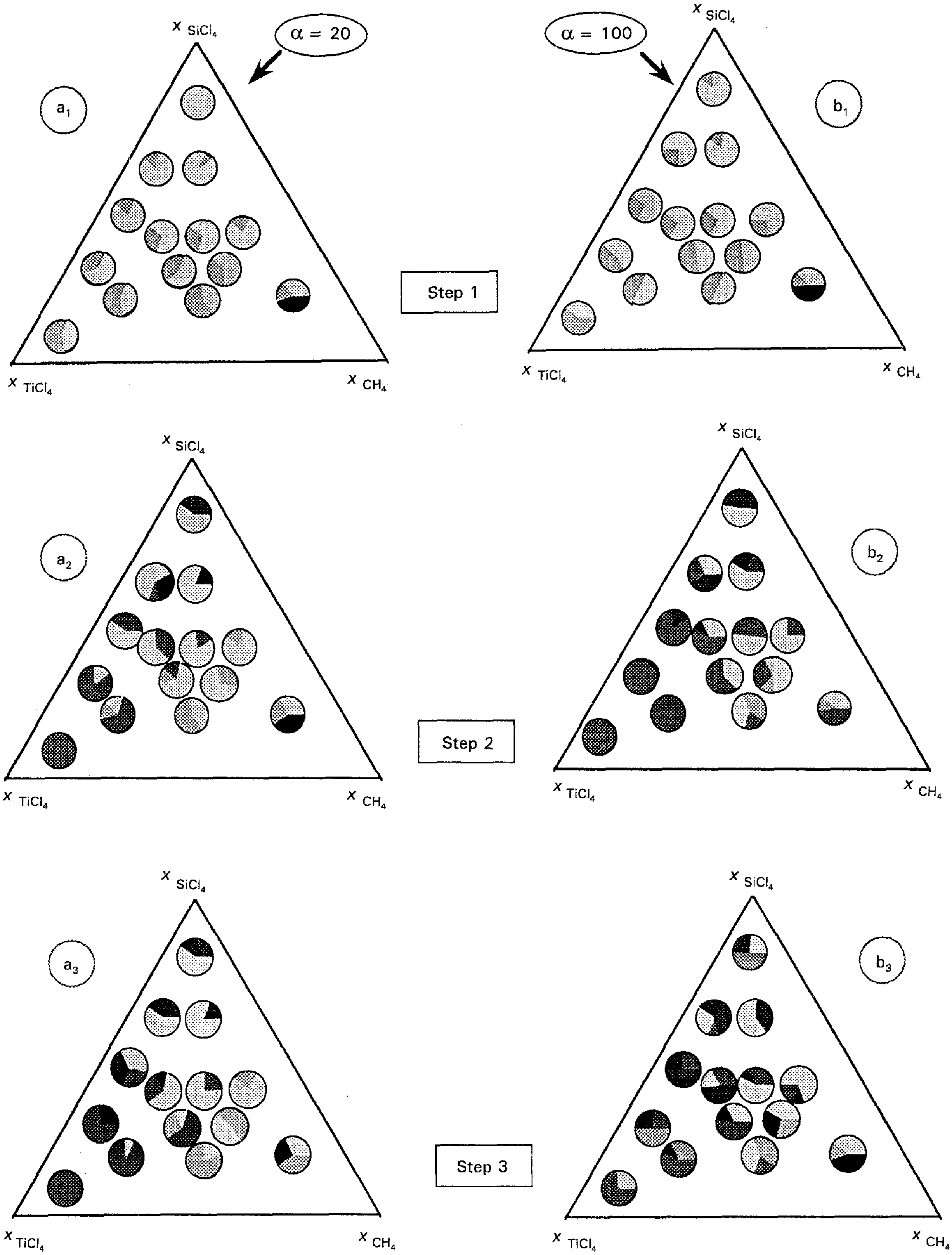

Figure 18 Successive equilibrium states, the complex solid obtained at any step being used as reactive substrate for the following step. Influence of the initial gaseous mixture for $T = 1273$ K, $P = 20$ kPa, $\alpha = 20$ and 100 and a first reactive substrate of carbon. For key to sectors see Table 2.

silicon substrate etching is only dependent on the ratio x_{TiCl_4}/x_{SiCl_4}. The silicon yield defined by

$$\eta_{Si} = 100\frac{n_{Si}^{eq} - n_{Si}^{in}}{n_{Si}^{in} + n_{SiCl_4}^{in}} \tag{32}$$

can be represented as a function of this ratio (Fig. 21). The silicon consumption is found to increase as the x_{TiCl_4}/x_{SiCl_4} ratio is raised.

As shown in Fig. 22, SiC–$TiSi_2$ mixtures are formed at equilibrium, with an excess of $TiSi_2$ for most of the initial compositions. SiC formation is favoured by an

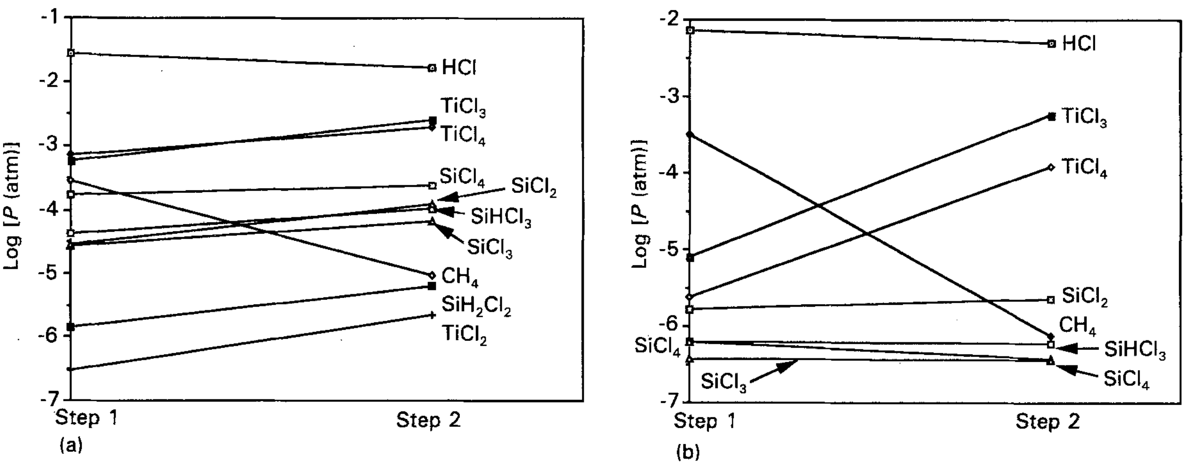

Figure 19 Equilibrium partial pressures of the gaseous species for the two steps of the deposition process on a reactive carbon substrate with (a) $\alpha = 20$, (b) $\alpha = 100$; $P = 20$ kPa, $T = 1273$ K, $x_{TiCl_4} = 0.8$, $x_{SiCl_4} = 0.1$, $x_{CH_4} = 0.1$.

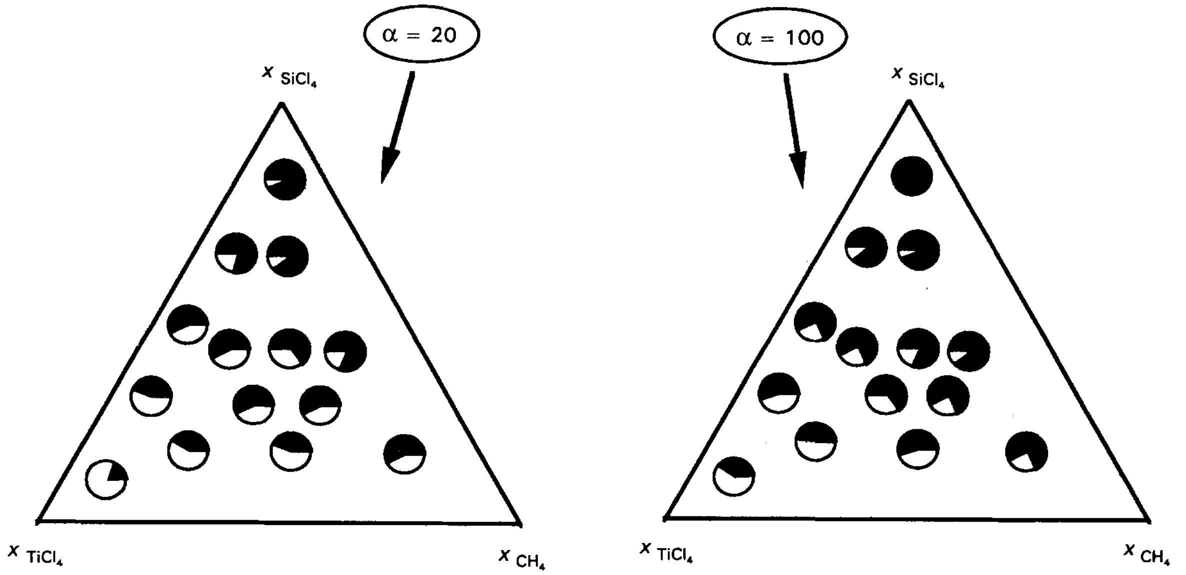

Figure 20 Influence of the initial gaseous mixture on the extent of the consumption of a silicon substrate at equilibrium for $T = 1273$ K, $P = 20$ kPa, $\alpha = 20$ and 100; n (Si) = 30 mol, n (SiCl$_4$) + n (TiCl$_4$) + n (CH$_4$) = 10 mol. Clear sectors represent the amount of consumed substrate and dark sectors the amount of unetched substrate.

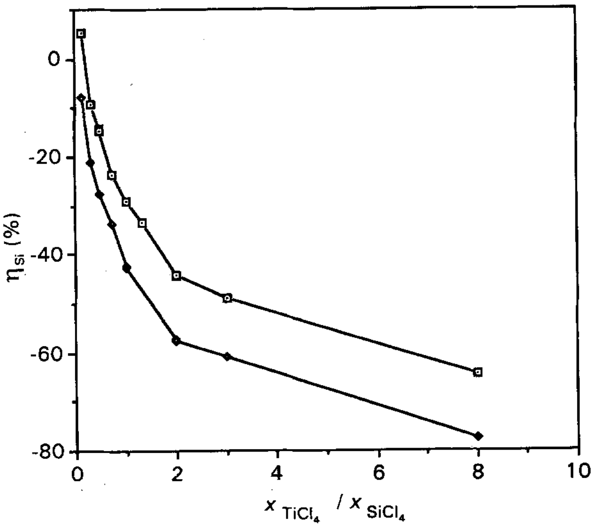

Figure 21 Influence of the ratio x_{TiCl_4}/x_{SiCl_4} on the silicon thermodynamic yields for $T = 1273$ K, $P = 20$ kPa, (◇) $\alpha = 20$, (□) $\alpha = 100$.

excess of CH$_4$ and to a lesser extent of SiCl$_4$. As a consequence, the following equations are thought to be involved in the silicon consumption process:

$$\mathrm{TiCl_4 + 2Si + 2H_2 \rightarrow TiSi_2 + 4HCl} \qquad (33)$$

$$\mathrm{CH_4 + Si \rightarrow SiC + 2H_2} \qquad (34)$$

Equation 33 is favoured by increase of x_{TiCl_4} and α, while Equation 34 is enhanced by rising x_{CH_4} and decreasing α ratio.

If a second series of equilibrium calculations is carried out as previously reported for a carbon substrate, Ti$_3$SiC$_2$ is formed in a relatively large composition range (Fig. 22a$_2$ and b$_2$). The solids formed in this second step can be considered as inert substrates, because in a third step the equilibrium gives rise to solids with compositions identical to those calculated for an inert substrate (Fig. 22a$_3$ and b$_3$). The initial compositions which favour pure Ti$_3$SiC$_2$ are rich in TiCl$_4$. Consequently, the gas-phase synthesis of this

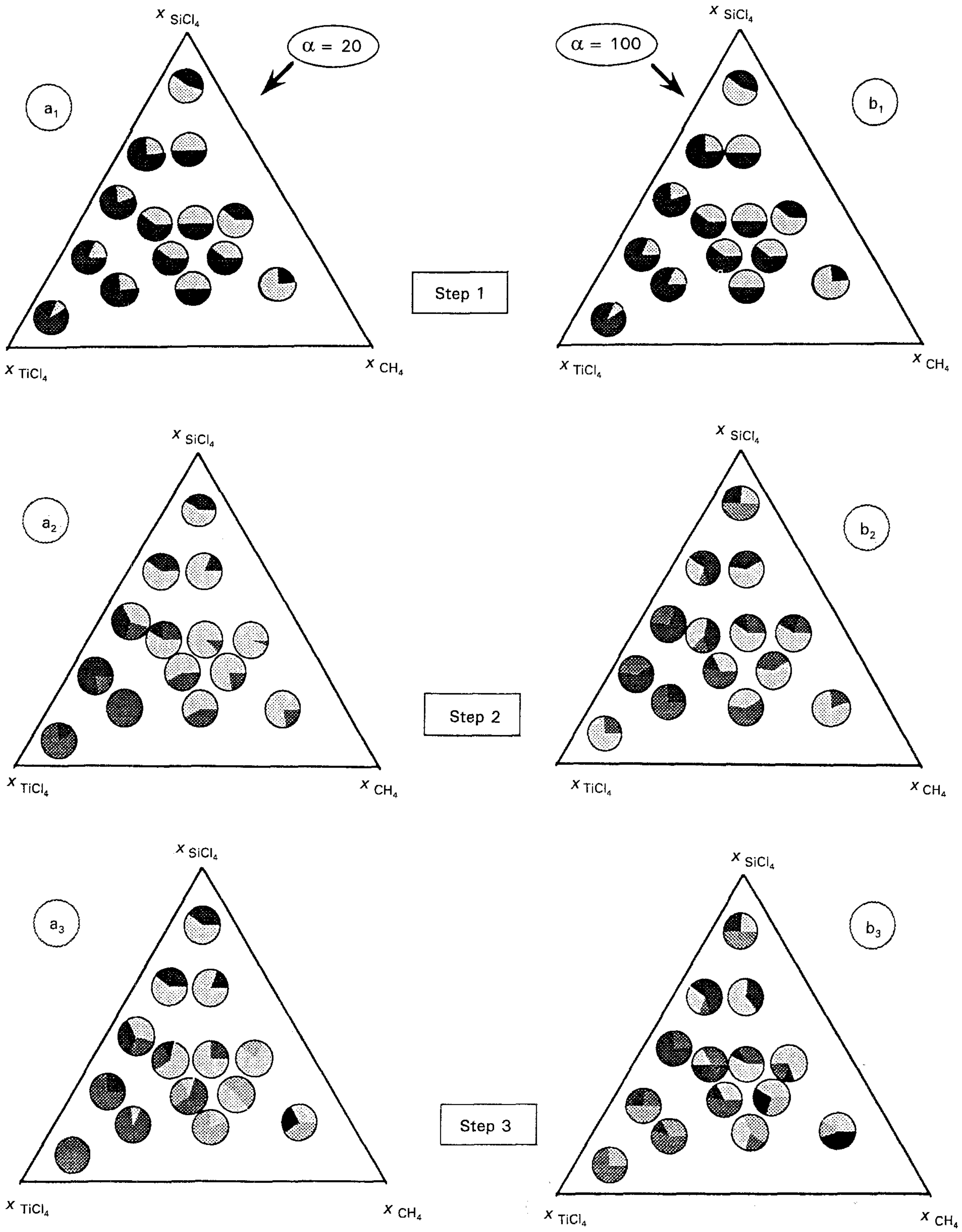

Figure 22 Successive equilibrium states, the complex solid obtained at any step being used as reactive substrate for the following step. Influence of the initial gaseous mixture for $T = 1273$ K, $P = 20$ kPa, $\alpha = 20$ and 100 and a first reactive substrate of silicon. For key to sectors see Table 2.

ternary phase on a silicon substrate occurs through an intermediate stage with $TiSi_2$ formation from reaction of $TiCl_4$ with Si (Equation 33).

Under the same conditions as for the carbon substrate, the equilibrium composition of the gas phase is reported in Fig. 23. For $\alpha = 20$, the first step corresponds to a total consumption of $TiCl_4$ and CH_4 and a production of HCl, $SiCl_4$, $SiCl_2$, $SiHCl_3$ and $SiCl_3$. Consequently, the etching of silicon does not result only from Reactions 33 and 34 but also from

$$Si + 4HCl \rightarrow SiCl_4 + 2H_2 \quad (35)$$

$$Si + 2HCl \rightarrow SiCl_2 + H_2 \quad (36)$$

$$Si + 3HCl \rightarrow SiHCl_3 + H_2 \quad (37)$$

$$Si + 3HCl \rightarrow SiCl_3 + \tfrac{3}{2}H_2 \quad (38)$$

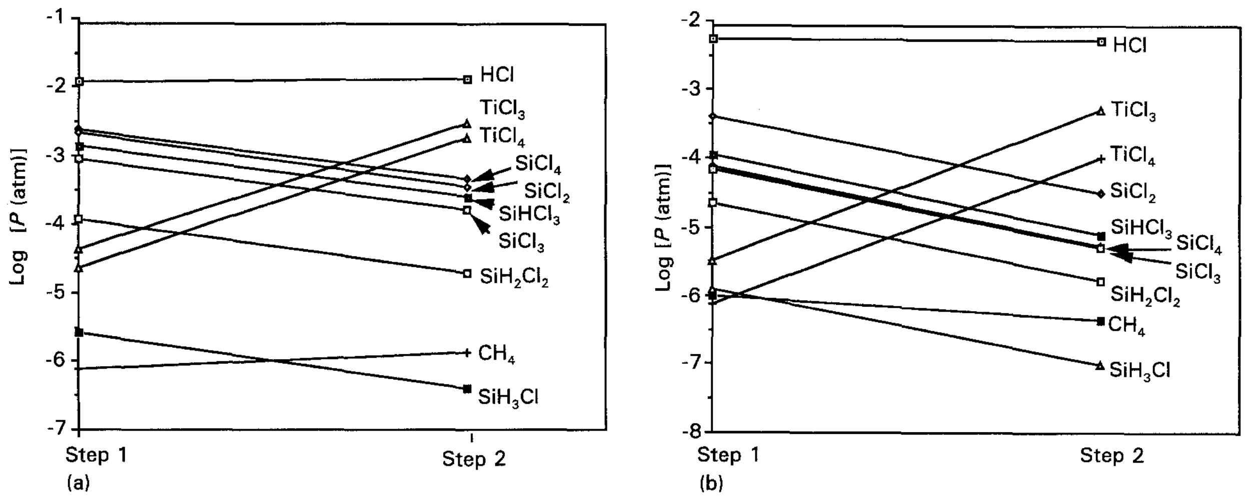

Figure 23 Equilibrium partial pressures of the gaseous species for the two steps of the deposition process on a reactive silicon substrate with (a) $\alpha = 20$, (b) $\alpha = 100$; $P = 20$ kPa, $T = 1273$ K, $x_{TiCl_4} = 0.8$, $x_{SiCl_4} = 0.1$, $x_{CH_4} = 0.1$.

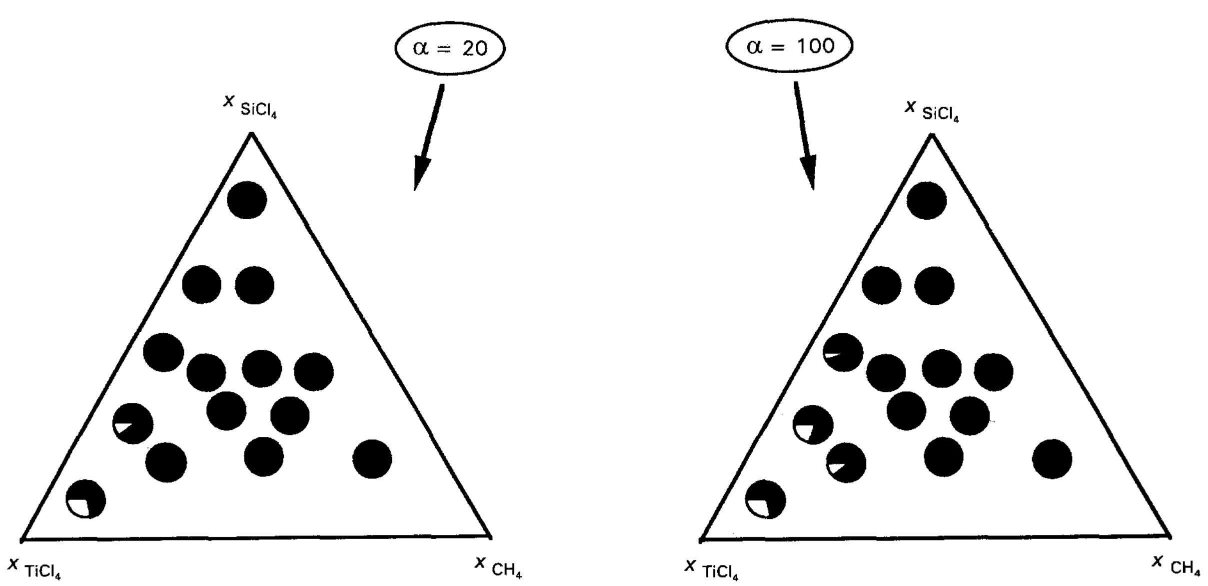

Figure 24 Influence of the initial gaseous mixture on the extent of the consumption of a silicon carbide substrate at equilibrium for $T = 1273$ K, $P = 20$ kPa, $\alpha = 20$ and 100; n (Si) = 10 mol, n ($SiCl_4$) + n ($TiCl_4$) + $n(CH_4)$ = 10 mol. Clear sectors represent the amount of consumed substrate and dark sectors the amount of unetched substrate.

In the second step, the equilibrium gas phase contains HCl, $TiCl_4$, $TiCl_3$ and small amounts of various silicon chlorides. Ti_3SiC_2 is obtained partly from the reaction of $TiCl_4$ on SiC, and partly from the reaction between $TiCl_4$, $SiCl_4$ and CH_4. For $\alpha = 100$, the subchlorides such as $TiCl_3$ and $SiCl_2$ are favoured with respect to other chlorides but the same reactions are involved in the Ti_3SiC_2 synthesis mechanism.

4.3. Silicon carbide substrate

The diagrams of Fig. 24 show the behaviour of an SiC substrate under the same conditions as for C and Si substrates previously investigated, i.e. $T = 1273$ K, $P = 20$ kPa, $\alpha = 20$ and 100. Silicon carbide is very slightly consumed only for a $TiCl_4$-rich precursor. In this case, Ti_3SiC_2 as a pure phase or in co-deposition with $TiSi_2$ can be obtained and a second step is needed to lead to results corresponding to the inert substrate, as shown in Fig. 25. In the other cases, i.e. for almost the whole initial composition range, SiC substrate can be considered as inert and the deposit composition previously reported is obtained from the first equilibrium calculations.

4.4. Discussion

Among the various substrates presently studied in the CVD system $TiCl_4$–$SiCl_4$–CH_4–H_2, carbon and silicon exhibit similar behaviour while silicon carbide is very different. Both C and Si substrates are highly consumed, the etching of Si being the highest one. Due to the reactivity of such substrates, the deposition of the ternary compound Ti_3SiC_2 can be obtained

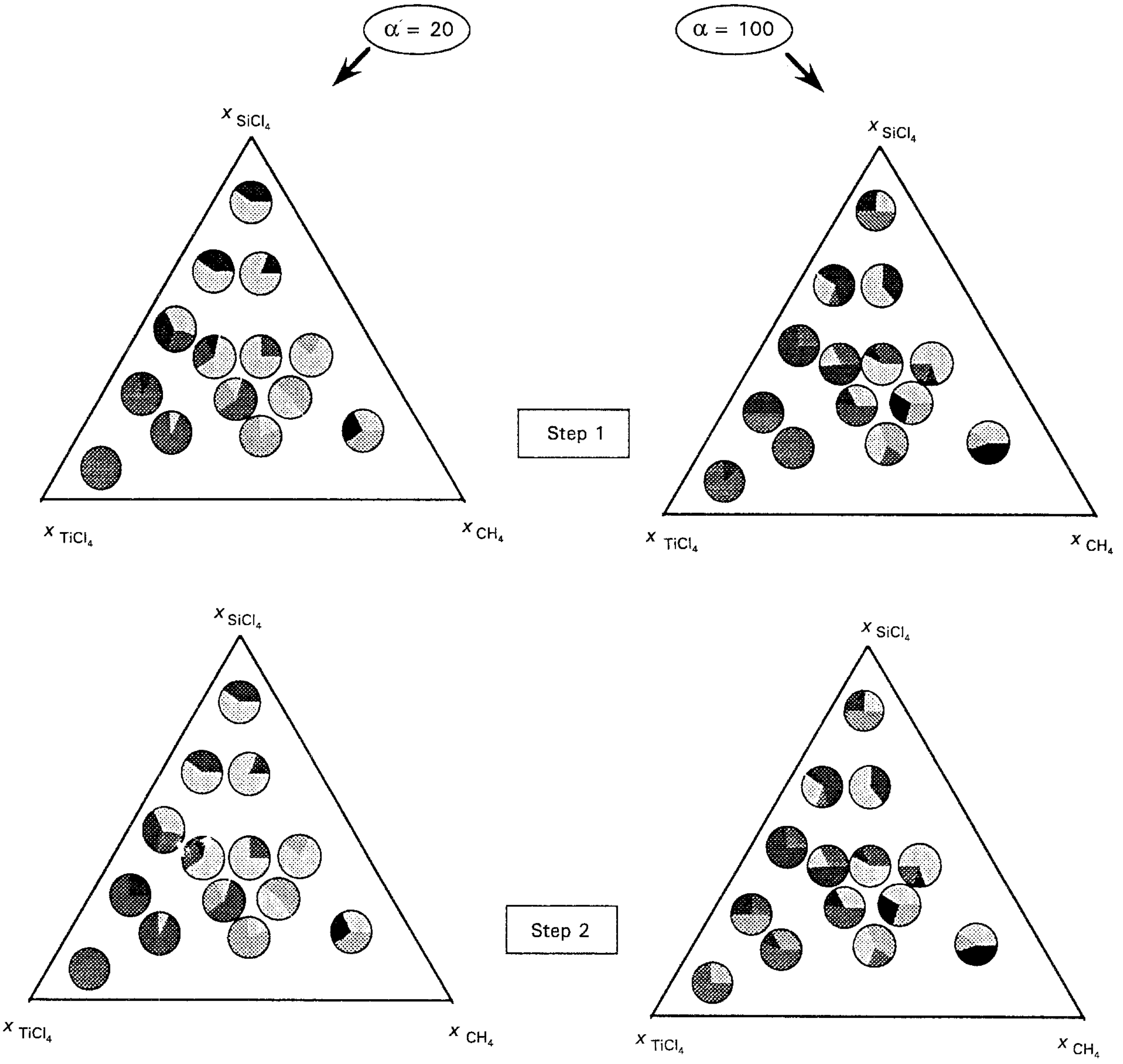

Figure 25 Successive equilibrium states, the complex solid obtained at any step being used as reactive substrate for the following step. Influence of the initial gaseous mixture for $T = 1273$ K, $P = 20$ kPa, $\alpha = 20$ and 100 and a first reactive substrate of SiC. For key to sectors see Table 2.

through an intermediate stage giving rise to TiC for carbon or $TiSi_2$ for silicon. The corresponding equations involved under well-chosen conditions could be

$$TiCl_4 + C + 2H_2 \rightarrow TiC + 4HCl \qquad (27)$$

and

$$TiCl_4 + 2Si + 2H_2 \rightarrow TiSi_2 + 4HCl \qquad (33)$$

In a second step, reactions such as TiC with $SiCl_4$ could give rise to Ti_3SiC_2. Conversely, this ternary compound can be obtained directly on a silicon carbide substrate with only a very slightly etching of this substrate. In this case, however, the initial composition range resulting in pure Ti_3SiC_2 deposition is rather narrow.

Acknowledgements

The authors wish to thank Société Européenne de Propulsion and CNRS for their support via a grant to C. Racault.

References

1. W. JEITSCHKO and H. NOWOTNY, *Mh. für Chem.* **98** (1967) 329.
2. J. J. NICKL, K. K. SCHWEITZER and P. LUXENBERG, *J. Less-Common Met.* **26** (1972) 335.
3. T. GOTO and T. HIRAI, *Mater. Res. Bull.* **22** (1987) 1195.
4. C. RACAULT, F. LANGLAIS and R. NASLAIN, *J. Mater. Sci.* **29** (1994).
5. T. GOTO and T. HIRAI, in proceedings of 10th International Conference on CVD, October, 1987, Honolulu, edited by G. W. Cullen (Electrochemical Society, Pennington, 1987) p. 1070.
6. M. TOUANEN, F. TEYSSANDIER and M. DUCARROIR, *J. Mater. Sci. Lett.* **8** (1989) 98.
7. S. SAMBASIVAN PhD dissertation, Arizona State University, Tempe, AZ, 1990
8. C. RACAULT, F. LANGLAIS and R. NASLAIN, *J. Mater. Sci.* **29** (1994) 000.
9. C. VAHLAS, P. Y. CHEVALIER and E. BLANQUET, *CALPHAD* **13**(3) (1989) 273.
10. C. VINCENT, J. DAZORD, J. BOUIX and C. BERNARD, *Thermochim. Acta* **147** (1989) 1.
11. F. TEYSSANDIER, M. DUCCAROIR and C. BERNARD, *CALPHAD* **8** (1984) 233.
12. B. URHENIUS, *ibid.* **8** (1984) 101.

13. M. HILLERT and L. I. SHAFFANSON, *Acta Chem. Scand.* **24** (1970) 3618.
14. L. KAUFMAN and H. BERNSTEIN, "Computer calculation of phase diagrams", (Academic, New York, 1970) p. 184.
15. W. J. J. WAKELKAMP, F. J. J. VAN LOO and R. METSELAAR, *J. Eur. Ceram. Soc.* **8** (1991) 135.
16. J. N. BARBIER and C. BERNARD, in Proceedings 15th *CALPHAD* Meeting, 7–11 June, 1986, Subergrange (England), p. 206.
17. H. HANNACHE, R. NASLAIN and C. BERNARD, *J. Less-Common Met.* **95** (1983) 221.
18. J. MINET, F. LANGLAIS, R. NASLAIN and C. BERNARD, *ibid.* **119** (1986) 219.

Received 3 December 1993
and accepted 19 January 1994